scientific reports

Check for updates

OPEN

Factor H-related 2 levels dictate FHR dimer composition

Bert R. J. Veuskens[1,2], Mieke C. Brouwer[1], Gerard van Mierlo[1], Judy Geissler[1], Karin van Leeuwen[1,4], Maaike Derlagen[4], Nadia C. H. Keijzer[4], Mark Hoogenboezem[1], Taco W. Kuijpers[1,3] & Richard B. Pouw[1,2,4]✉

Factor H-related (FHR) protein 1 and 2 form dimers resulting in FHR-1 and -2 homodimers, and FHR-1/2 heterodimers. Dimerization is hypothesized to further increase their antagonistic function with complement regulator factor H (FH). So far, only FHR-1 homodimers and FHR-1/2 heterodimers could be quantified in a direct way. With the reported genetic associations between *CFHR2* and complement-related diseases such as age related macular degeneration and C3-glomerulopathy, direct assessment of FHR-2/2 levels determining the dimer distribution of FHR-1 and -2 is needed to further elucidate their role within complement regulation. Therefore, novel in-house generated FHR-2 antibodies were used to develop a specific ELISA to enable direct quantification of FHR-2 homodimers. Allowing for the first time the accurate measurement of all FHR-1 and -2 containing dimers in a large cohort of healthy donors. By using native FHR-1 and -2 or deficient plasma, we determined the stability, kinetics and distribution of FHR-1 and -2 dimers. Additionally, we show how genetic variants influence dimer levels. Our results confirm a rapid, dynamic, dimer formation in plasma and show FHR-1/2 dimerization rearches a distribution equilibrium that is limited by the relative low levels of FHR-2 in relation to its dimerization partner FHR-1.

Keywords Complement system, FHR-1, FHR-2, Dimerization

The complement system, an integral component of innate immunity, serves as a primary defence mechanism by effectively eliminating invading pathogens. To safeguard healthy host cells from damage, the complement system is tightly regulated[1,2]. One of the main complement regulators is factor H (FH), playing a key role in regulating complement activation via the alternative pathway (AP), both in fluid phase and on cellular surfaces[3]. In addition to FH, the *CFH* locus also encompasses five FH paralogues, referred to as the FH-related (FHR) proteins (FHR-1 to -5)[4]. Like FH, the FHRs consist of multiple complement control protein (CCP) domains and share a high degree of sequence similarity with FH and among each other. This similarity is likely originating from non-allelic homologous recombination events of the *CFH* gene[5,6]. However, only the surface recognition rather than the regulatory CCP domains of FH are conserved within the FHRs. As a result, the FHR proteins are hypothesized to act as antagonists of FH by competing for binding to shared ligands (*e.g.* C3b, heparan sulphate, sialic acids) rather than directly regulating complement[7,8]. Consequently, the FHRs may act as localized fine-tuners of the AP by interfering with the regulatory functions of FH[9].

Of the FHRs, FHR-2 is the smallest (24/29 kDa) and most elusive member. FHR-2 shares a high degree of similarity with FHR-1 and -5 (Fig. 1a). Like FHR-1 and -5, FHR-2 contains a dimerization motif within its first two N-terminal CCP domains. The residues Tyr34, Ser36 and Tyr39 (mature protein numbering) were identified to play a crucial role in dimer formation, enabling FHR-1, -2, and FHR-5 to assemble into non-covalent homo- and/or heterodimers in a head-to-tail orientation[10]. As such, FHR-2 is primarily found in circulation as a heterodimer with the more abundant FHR-1[11]. While FHR-2 homodimers do exist, directly quantifying their levels is challenging due to the prevalence of FHR-1/2 heterodimers and the lack of sufficiently sensitive and FHR-2-specific reagents[11]. Although the dimerization motif is conserved among FHR-1, -2, and FHR-5, there is some controversy regarding whether FHR-5 can form heterodimers in healthy individuals[10,11]. Previous studies have demonstrated dimerization affects the avidity of FHR-1, -2 and FHR-5 to their surface-bound ligands, likely increasing their ability to compete with FH and influence complement regulation[7,10–13]. Consequently,

[1]Sanquin Research and Landsteiner Laboratory of the Amsterdam University Medical Centers, University of Amsterdam, Plesmanlaan 125, 1066 CX Amsterdam, The Netherlands. [2]Amsterdam Institute for Immunology and Infectious Diseases, Inflammatory Diseases, Amsterdam, The Netherlands. [3]Department of Paediatric Immunology, Rheumatology and Infectious Diseases, Emma Children's Hospital, AUMC, University of Amsterdam, 1105 AZ Amsterdam, The Netherlands. [4]Sanquin Diagnostic Services, 1066 CX Amsterdam, The Netherlands. ✉email: richard.pouw@sanquin.nl

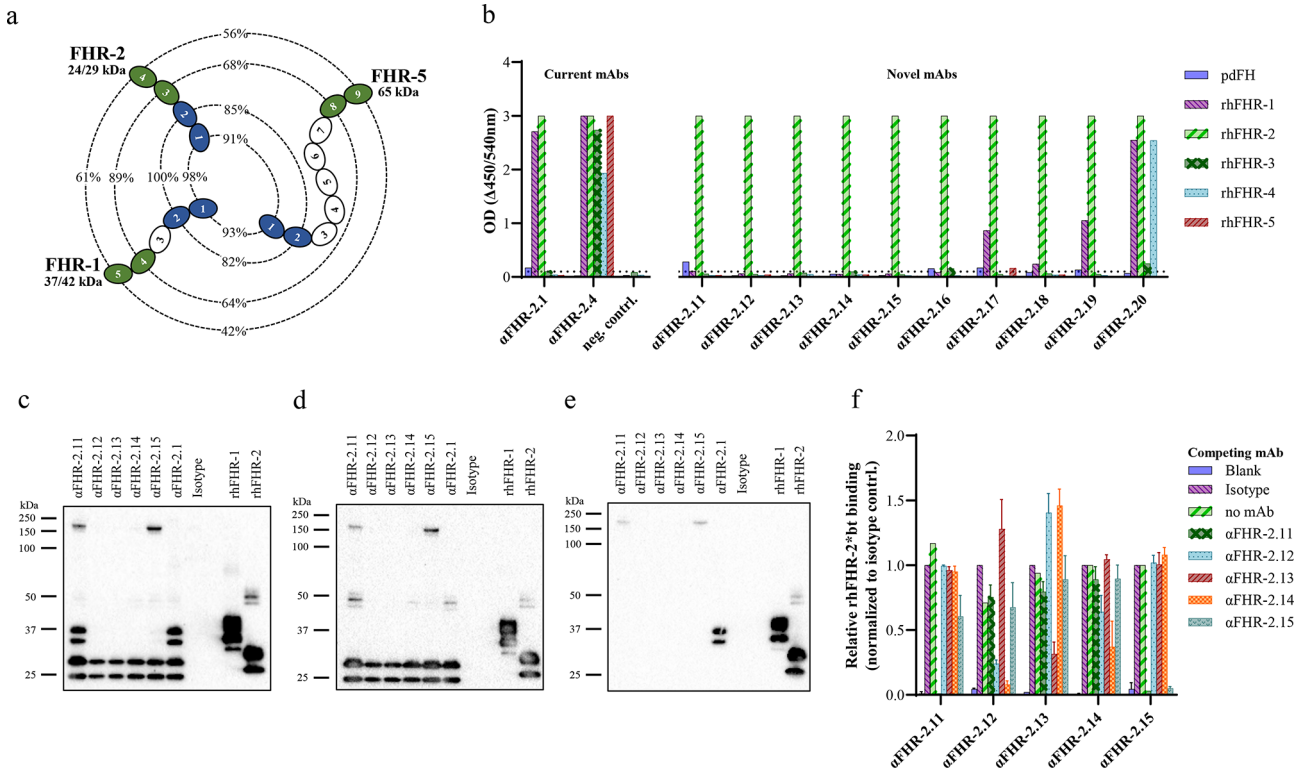

Fig. 1. Characterization of FHR-2 monoclonal antibodies (mAbs). (**a**) An overview illustrating the genetic similarity between FHR-1, -2, and FHR-5. (**b**) Cross-reactivity analysis of the αFHR-2 mAbs. Wells were coated with the indicated αFHR-2 mAb and incubated with biotinylated plasma-derived FH (pdFH) or recombinant human FHR (rhFHR) proteins (10 nM). Current non-specific αFHR-2 mAbs (αFHR-2.1, αFHR-2.4) and an irrelevant isotype mAb (neg. contrl.) were included as controls[11]. Absorption levels above 0.1 (dotted line) were considered indicative of cross-reactivity. Some test conditions resulted in absorption levels exceeding the upper limit of quantification, set at 3.0. (**c**–**e**) Western blot analysis of immunoprecipitation using αFHR-2.11 to αFHR-2.15 in normal human serum (**c**), *CFHR3/CFHR1* deficient serum (determined via MLPA) (**d**), and serum deficient for FHR-2 (previously determined via gene sequencing) (**e**)[11]. All three immunoblots were stained using αFHR-2.1 (cross-reactive for FHR-1 and -2) to verify specificity for native FHR-2 and exclude cross-reactivity for native FHR-1. (**f**) Competition ELISA including selective αFHR-2 mAbs. Biotinylated rhFHR-2 (0.1 µg/mL) was pre-incubated with αFHR-2 mAbs (10 µg/mL) for twenty minutes before adding to the ELISA plates coated with indicated mAbs. Binding of biotinylated rhFHR-2 is expressed as relative binding of biotinylated rhFHR-2 in the presence of an isotype control. Bars represent the mean of two independent replicates with error bars indicating the SD. ELISAs and Western blots are representatives of three independent experiments.

differences in ligand specificity and affinity between the FHRs and the dimer distribution could influence their competition with FH.

Additionally, FHR levels vary within the population, which in turn also could play a role in the overall complement regulation by FH[14,15]. For FHR-1 this variability is predominantly genetically determined, but environmental factors and various disease states can also contribute to this fluctuation[14]. The common *CFHR3/CFHR1* and the less common *CFHR1/CFHR4* deletion were found to substantially impact the plasma concentrations of FHR-1 and subsequently the distribution of the dimeric species[11]. A complete lack of FHR-1 caused by the homozygous deletion of *CFHR3/CFHR1* was reported to be protective for AMD, with elevated FHR-1/1 and -1/2 levels being associated with advanced stages of the disease[16,17]. Furthermore, the common single nucleotide polymorphisms (SNPs) rs4085749 (c.420C > T, p.(Arg141Phefs*12) and certain low-frequency SNPs in *CFHR2* were previously hypothesized to impact FHR-2 levels[15,16,18]. Like FHR-1, elevated inferred levels of FHR-2 were previously associated with advanced AMD[16]. Furthermore, above mentioned low frequency *CFHR2* mutations were linked with lower inferred FHR-2 levels, which in turn showed to confer for AMD protection[16]. A potential shift in the FHR-1 and -2 dimers could potentially explain this reported association.

Our group previously used a theoretical approach to estimate FHR-2 homodimer levels[11,19–21]. These calculations were based on the measured levels of FHR-1/1 and -1/2, assuming that FHR dimerization reaches a distribution equilibrium. This analogy to classic genetics, such as Hardy–Weinberg equilibrium, reflects the dynamic process of FHR dimerization, where dimer formation is unbiased, and free monomer exchange occurs between the dimers, solely governed by their affinity, stability and relative abundance[11,22]. However, testing this

theoretical approach and validating these reported associations and predictions by direct FHR-2/2 measurement is needed.

In this study, we generated novel mouse monoclonal antibodies (mAbs) utilizing a relatively unique part of FHR-2 as target antigen. Use of these mAbs resulted in the development of a specific FHR-2 homodimer ELISA, allowing, in combination with our previously established FHR-1/1 and -1/2 ELISAs, quantification of all FHR-1 and -2 dimer species[11]. Furthermore, we determined the predicted effects of known SNPs on FHR-2 levels and show their impact on dimer distribution[18,21]. Finally, we studied whether the distribution equilibrium does apply on FHR-1 and -2 dimerization in a healthy donor population. By establishing the FHR-1 and -2 dimer distribution during health we aim to better understand the role of these proteins within the complement system and related diseases.

Results

Antibody characterisation: identification of five highly FHR-2 specific monoclonal antibodies

To minimize the chance of obtaining antibodies cross-reactive for FHR-1 and -5 (Fig. 1a), only FHR-2 CCP3-4, being the most unique part of FHR-2, was recombinantly expressed in HEK293F cells and subsequently used for mouse immunisation. Full length wild type recombinant human FHR-2 (rhFHR) was used to screen the cultured hybridoma's. Ten hybridoma clones, producing mouse anti-human FHR-2 IgG1 kappa antibodies, were identified (Table 1). Five clones, named αFHR-2.11 to αFHR-2.15, were found to be all highly specific for rhFHR-2 (Fig. 1b). The remaining five clones (αFHR-2.16 to αFHR-2.20) cross-reacted with other members of the FH protein family (Table 1, Fig. 1b).

Cross-reactivity towards native FHR-1 was further assessed via immunoprecipitation (IP) for clones αFHR-2.11 to αFHR-2.15. As expected, and due to the presence of FHR-1/2 heterodimers, both FHR-1 (37/42 kDa) and -2 (24/29 kDa) were precipitated from normal human serum (NHS) (Fig. 1c) when detecting with a FHR-1, -2 cross-reactive mAb. Surprisingly, αFHR-2.12 to -2.14 did not co-precipitate FHR-1 in NHS, suggesting a selective precipitation of FHR-2 homodimers. To exclude cross-reactivity with native FHR-1, IP using serum deficient for FHR-1 (Fig. 1d), as validated by MLPA (Table 3), resulted in a single signal for FHR-2. Additionally, when using donor serum lacking FHR-2 (Fig. 1e) as previously identified by van Beek et al.[11] (Table 4), no FHRs were being detected[11]. For all three serum pools, a signal around 150 kDa was observed for αFHR-2.11 and αFHR-2.15. To exclude cross-reactivity with FH, IP of those mAbs in FHR-1 and -2 deficient serum were stained for FH (supplemental Fig. S1a) which excluded FH cross-reactivity. In addition, αFHR-2.11, -2.14, -2.15 and αFHR-2.1 showed three bands around 50 kDa in both NHS and FHR-1 deficient serum, but not in FHR-2 deficient serum. A potential explanation for this could be the presence of FHR-2 homodimers in NHS and FHR-1 deficient serum that are not fully disintegrated during the immunoblotting process. Bands at similar heights are also visible in the rhFHR-2 control. In summary, these results agree with the findings of the ELISA and show αFHR-2.11 to αFHR-2.15 are highly FHR-2 specific mAbs.

Next, all ten αFHR-2 mAbs were characterized for epitope competition (Table 1, Fig. 1f). Among them, αFHR-2.11 and αFHR-2.15 were found to compete for the same or overlapping epitopes, as they prevented binding of rhFHR-2 to each other. The same observation was made for αFHR-2.12, -2.14 and for αFHR-2.19, -2.20. αFHR-2.16, -2.17, and αFHR-2.18 exhibited similar blocking effects as αFHR-2.11, -2.15. However, as they show differential cross-reactivity with members of the FH family, suggesting different epitopes, their blocking effect is likely attributed to steric hindrance rather than direct competition for epitope binding.

αFHR-2.11 can be used to specifically detect FHR-2/2 homodimers

Using the same principle as our previously published FHR-1 homodimer ELISA, *i.e.* only an FHR-2 homodimer presents a single FHR-2 epitope twice, we developed a sandwich ELISA (supplemental Fig. S1b) using the same mAb as coat and detection[11]. To this end, FHR-2 selective mAbs were tested in NHS to identify the most suitable antibody (Fig. 2a). Among them, only αFHR-2.11 successfully detected FHR-2 homodimers. In contrast to NHS, serum deficient in FHR-1 showed higher optical densities, suggesting that in the absence of FHR-1 a higher level of FHR-2 homodimers is present.

Clone name	Cross-reactivity (ELISA)	Immunoprecipitation	Competition
αFHR-2.11	None	FHR-1, FHR-5	2.15, 2.16, 2.17, 2.18
αFHR-2.12	None	None	2.14
αFHR-2.13	None	None	None
αFHR-2.14	None	None	2.12
αFHR-2.15	None	FHR-1	2.11, 2.16, 2.17, 2.18
αFHR-2.16	FHR-3	n.d	2.11, 2.15, 2.17, 2.18
αFHR-2.17	FHR-1	n.d	2.11, 2.15, 2.16, 2.18
αFHR-2.18	FHR-1	n.d	2.11, 2.15, 2.16, 2.17
αFHR-2.19	FHR-1	n.d	2.20
αFHR-2.20	FHR-1, FHR-3, FHR-4	n.d	2.19

Table 1. FHR-2 monoclonal antibody characteristics. All antibodies are of mouse IgG1 isotype with a kappa light chain and bind an epitope located in CCP3-4 of FHR-2. n.d: not determined.

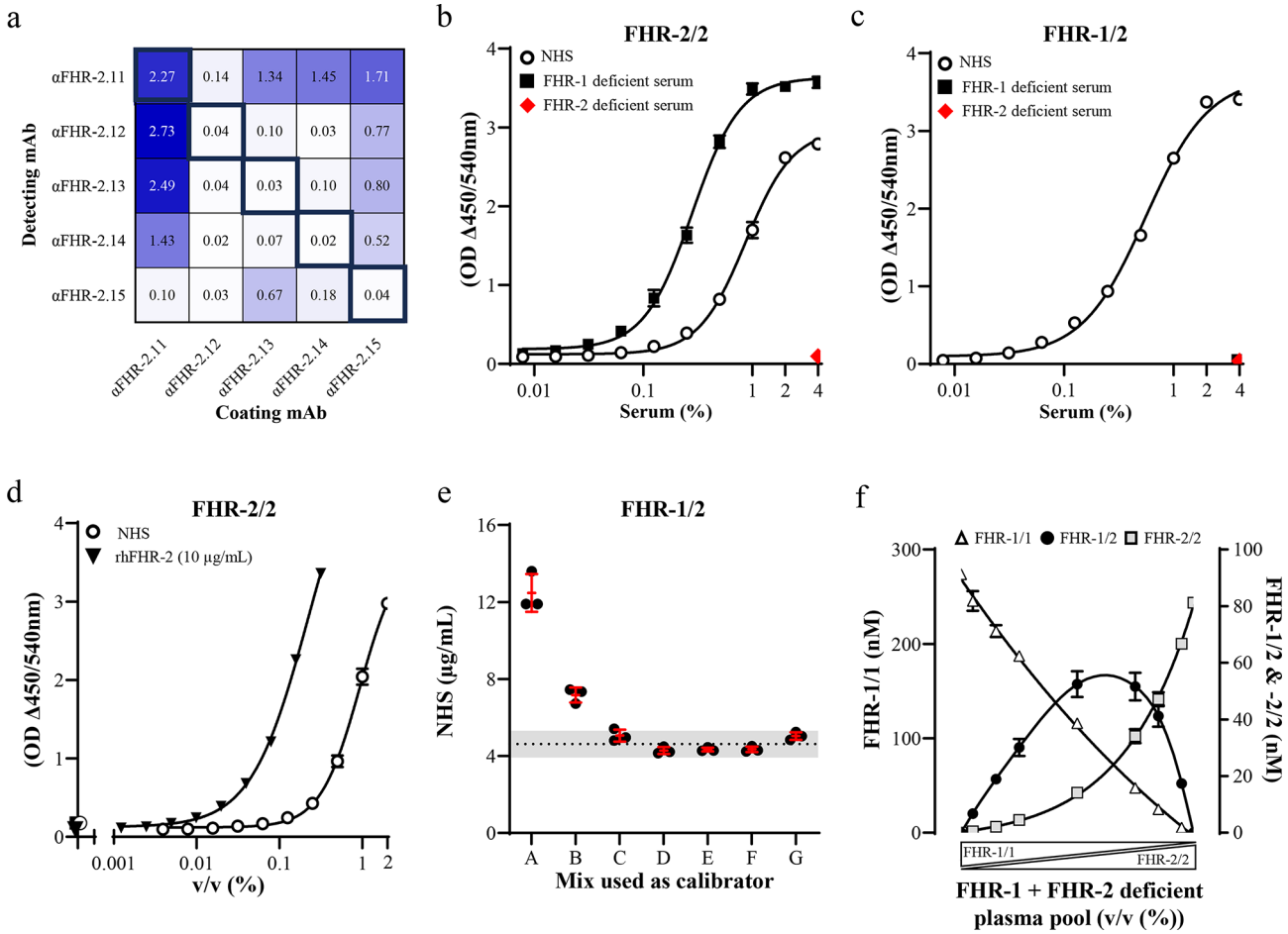

Fig. 2. ELISA validation and calibration. (**a**) Selection of monoclonal antibody (mAb) sandwich combination to enable detection of FHR-2/2 homodimers in normal human serum (NHS). Combinations of the same mAb (bolt bordered squares) are of interest based on the principal only a homodimer presents a single FHR-2 epitope twice. ELISA plates were coated with a FHR-2 specific αFHR-2 mAb and incubated with 20% (v/v) NHS. Next, bound FHR-2 was detected using indicated biotinylated αFHR-2 mAb. Absorption levels above 0.1 were considered indicative of antigen detection. Validation of FHR-2/2 (**b**) and FHR-1/2 (**c**) assay specificity using NHS and serum deficient for FHR-1 or -2. The FHR-2 specific αFHR-2.11 mAb was coated on ELISA plates and incubated with either NHS and serum deficient for FHR-1 or -2 (4%, (v/v)). Next, bound target protein was detected using biotinylated αFH.02 (αFH mAb cross-reactive with FHR-1) or αFHR-2.11 for FHR-1/2 and -2/2 dimers, respectively[23]. (**d**) FHR-2/2 assay calibration of an NHS standard using rhFHR-2. For the calibration of the FHR-1/2 ELISA, seven mixes with different volumetric ratios (mix A: 95–5%, B: 85–15%, C: 75–25%, D: 50–50%, E: 25–75%, F: 15–85%, G: 5–95% (v/v)) of a plasma deficient in FHR-2 or -1 respectivaly were mixed and incubated at 37 °C for six hours to allow the formation of FHR-1/2 heterodimers. (**e**) NHS standard pool calibrated for FHR-1/2 using each mix as standard. FHR-1/2 levels in each mix were based on the average decline in FHR-1/1 and -2/2. Dotted line represents the mean of mix C-G with the grey area indicating the mean ± 15%. (**f**) Levels of all three FHR-1 and -2 dimer species in each mix (start concentration FHR-1/1: 273.84 nM; start concentration FHR-2/2: 81.20 nM) after incubation at 37 °C. (**a**–**d**) n = 3, representative is shown. (**b**–**f**) Symbols represent mean of multiple measurements with error bars indicating the SD.

As FHR-1 and -5 also form homodimers that present a single epitope twice, ELISA specificity for FHR-2/2 was further challenged. FHR-2 specificity of αFHR-2.11 was tested in the presence of high amounts of NHS and serum deficient for FHR-1 or -2 (20% (v/v)) in combination with various αFHR-1 and αFHR-5 mAbs (supplemental Fig. S1d). No protein was detected when using either αFH.02 (αFH mAb cross-reactive with FH and FHR-1) or two specific αFHR-5 mAbs (αFHR-5.1, αFHR-5.4) in combination with αFHR-2.11, again confirming assay specificity for FHR-2/2[11,23].

αFHR-2.11 enables optimal detection of FHR-1/2 heterodimers

The previously developed FHR-1/2 heterodimer ELISA uses αFH.02, an αFH mAb cross-reactive for FHR-1, as capture antibody[11]. This approach captures not only FHR-1/2 heterodimers but may also be affected by the more abundant FH and FHR-1 homodimers. Therefore, a novel FHR-1/2 ELISA (supplemental Fig. S1c) was

developed, using αFHR-2.11 and αFH.02 as the capture and the detection mAb respectively. Like the FHR-2/2 ELISA, assay specificity was verified using NHS and deficient sera (Fig. 2c). Protein could only be detected in NHS where both FHR-1 and -2 are present as FHR-1/2 heterodimers. Conversely, sera lacking in either FHR-1 or -2 exhibited no signal, confirming assay specificity for FHR-1/2.

Calibration of the FHR-2/2 and -1/2 dimer ELISAs

For the FHR-2/2 ELISA, rhFHR-2 was used to calibrate our NHS standard, containing 1.36 µg/mL (25.64 nM, based on a molecular weight of 53 kDa) FHR-2/2 (Fig. 2d).

To calibrate our novel FHR-1/2 ELISA, we could not use rhFHR-1/2, as due to the dynamic nature of dimerization, it is unknown how much of rhFHR-1/2 is formed upon mixing rhFHR-1/1 and -2/2. To overcome this, we used the here described FHR-2/2 ELISA and the previously described FHR-1/1 ELISA to first establish the level of FHR-2/2 and FHR-1/1 in a plasma pool of *CFHR3/CFHR1* deficient donors and two pooled donors deficient for FHR-2[11]. These plasma samples were specifically selected to be deficient in either FHR-1 or FHR-2. The FHR-1 deficient plasma served as a source of FHR-2/2, while the FHR-2 deficient plasma provided FHR-1/1. Consequently, each pool contained only FHR-1/1 or FHR-2/2, respectively, with no FHR-1/2 heterodimers present. Next, due to the dynamic nature of FHR-1 and -2 dimerization, FHR-1/2 heterodimers were formed by mixing these plasmas at fixed volumetric ratios (mix A: 95–5%, B: 85–15%, C: 75–25%, D: 50–50%, E: 25–75%, F: 15–85%, G: 5–95% (v/v) FHR-2 deficient and *CFHR3/CFHR1* deficient plasma, respectively) followed by incubation at 37 °C for six hours. After incubation, remaining levels of FHR-1/1 and -2/2 were again quantified with the respective ELISAs and compared to the starting concentration of FHR-1/1 and -2/2 of each mix (Table 2). The difference in homodimer levels was compared, showing a similar decline in FHR-1/1 and FHR-2/2 homodimers in the mixes C to G. Next, we took the average of the decline in FHR-1/1 and -2/2 and calculated the formed FHR-1/2 levels in each mix (Table 2), which in turn was used as calibrator for the FHR-1/2 levels in all other mixes (supplemental Fig. S1e) and the NHS standard (Fig. 2e). The resulting FHR-1/2 levels were highly consistent within mixes C-G and the NHS standard. For mixes A and B, the resulting FHR-1/2 levels were relatively high and deviated substantially from the other mixes. This was likely due to the relative decline of FHR-1/1 (between 5 and 8%, Table 2) in these mixtures falling within or close to the normal assay variation (CV = 11%) as determined by the coefficient of variation (CV) from three controls measured at least 20 times. As a result, the decrease in FHR-1/1 could not be accurately quantified. Notably, in mixes A and B, the measured FHR-1/2 levels did correspond with the decline in FHR-2/2 (Table 2). Using mix C to G, the NHS standard was calibrated to contain 4.62 µg/mL (± 0.39 µg/mL corresponding to 70.00 ± 5.95 nM, 66 kDa) FHR-1/2 heterodimers (Fig. S2f). Finally, with all dimers now quantified within the mixed samples, the formation of FHR-1/2 and the decline in FHR-1 and -2 homodimers as a result of different ratios of FHR-1/1 and -2/2 could be modelled (Fig. 2f). This showed that FHR-1/2 formation increases with a maximum at a molar ratio of 2.25 FHR-1/1 over FHR-2/2, reflecting the normal ratio of FHR-1 and -2 in healthy human plasma.

Insights in FHR-1 and FHR-2 dimerization

Now equipped with the tools to specifically detect FHR-2 and directly quantify all FHR-1 and -2 dimers, we further investigated their kinetics and stability. First, we showed that upon incubation at 37 °C of equimolar amounts of FHR-1 and -2, a rapid formation of FHR-1/2 heterodimers is observed (Fig. 3a). This indicates dimerization of FHR-1 and -2 is a dynamic process that occurs in plasma and reaches an equilibrium after three hours. The stability of FHR-1 and -2 dimers was investigated under varying pH conditions and increasing sodium chloride concentrations. When NHS was incubated at different pH levels (Fig. 3b), lower homodimer levels were observed for FHR-1/1 between pH 6.5–8.0 and for FHR-2/2 between pH 6.5–7.5. Conversely, FHR-1/2 levels remained consistent across the entire pH range. Upon increasing sodium chloride concentrations (Fig. 3c, supplemental Fig. S2c), FHR-1/1 levels exhibited a stronger decline compared to FHR-1/2 (0.25 M: $p < 0.0001$; 0.5 M: $p = 0.035$: 1.0 M: $p = 0.0097$) and -2/2 (0.25 M: $p < 0.0001$; 0.5 M: $p = 0.0096$; 1.0 M: $p < 0.0001$) in the range between 0.25 and 1.0 M sodium chloride. Both FHR-1/2 and FHR-2/2 levels demonstrated a similar decreasing trend until reaching a concentration of 2 M sodium chloride, which showed significantly lower levels

Sample	% Pool 1 (%, v/v)	% Pool 2 (%, v/v)	FHR-1/1 measured in sample			FHR-2/2 measured in sample			Formed FHR-1/2 (theoretical)		
			Start	After	Delta (Δ)	Start	After	Delta (Δ)	Based on ΔFHR-1/1	Based on ΔFHR-2/2	Average
Pool 1: FHR-2 def.	–	–	273.84	-	–	0.00	–	–	–	–	–
Pool 2: *CFHR3/CFHR1* def.	–	–	0.00	-	–	81.20	–	–	–	–	–
Mix A	95	5	260.15	245.57	− 14.58	4.06	0.51	− 3.55	29.16	7.11	18.13
Mix B	85	15	232.76	213.50	− 19.26	12.18	2.10	− 10.08	38.52	20.17	29.35
Mix C	75	25	205.38	187.34	− 18.04	20.30	4.50	− 15.80	36.08	31.60	33.84
Mix D	50	50	136.92	115.99	− 20.93	40.60	14.16	− 26.43	41.86	52.87	47.36
Mix E	25	75	68.46	47.64	− 20.82	60.90	34.15	− 26.75	41.65	53.49	47.57
Mix F	15	85	41.08	24.81	− 16.27	69.02	47.17	− 21.85	32.53	43.69	38.11
Mix G	5	95	13.69	4.37	− 9.32	77.14	66.73	− 10.41	18.65	20.81	19.73

Table 2. Calculation table used for calibrating FHR-1/2 ELISA. Levels are reported in nM and are an average of three independent measurements. def.: deficient.

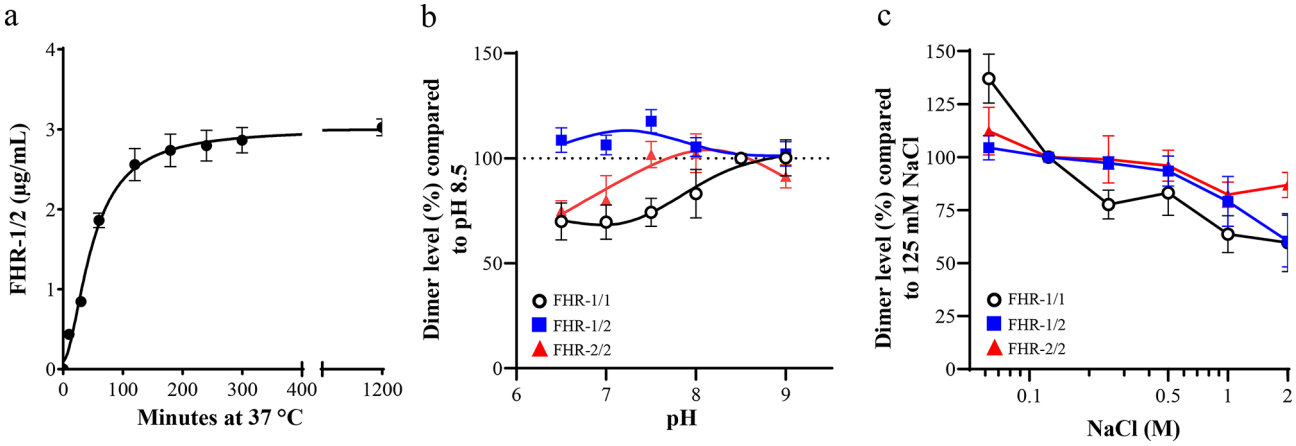

Fig. 3. Insights into FHR-1 and -2 dimerization. (**a**) FHR-1/2 ELISA was used to show the rapid formation of FHR-1/2 dimers over time when incubating equimolar amount of FHR-1 and FHR-2 at 37 °C. A plasma pool deficient in FHR-1 or FHR-2 was used as source for FHR-2/2 and FHR-1/1 respectively. FHR-1/2 levels were measured at 4 °C to halt further dimer formation. (**b**) Impact of pH on the stability of FHR-1 and -2 dimers. Normal human serum (NHS, 3% v/v) was incubated at the indicated pH using an isotonic 40 mM BisTrispropane buffer. pH 8.5 was used as reference, resembling the pH of the in-house dimer ELISAs. (**c**) Impact of sodium chloride on dimer stability. NHS (3%, (v/v) was incubated with increasing concentrations of sodium chloride ranging from 0.0625–2 M. 125 mM NaCl was used as a 100% reference. Symbols represent mean of three separate measurements with error bars indicating the SD.

	CFHR3	*CFHR1*	*CFHR4*	*CFHR2*	*CFHR5*	n of 201(%)
Gene copies	2	2	2	2	2	65 (32.34)
	2	2	n.d	2	2	67 (33.33)[a]
Variations	0	0	2	2	2	4 (1.99)
	0	0	n.d	2	2	4 (1.99)[a]
	1	0	1	2	2	1 (0.50)
	1	1	2	2	2	23 (11.44)
	1	1	n.d	2	2	33 (16.42)[a]
	1	2	3	2	2	1 (0.50)
	2	1	1	2	2	1 (0.50)
	2	1	n.d	2	2	1 (0.50)[a]
	3	3	n.d	2	2	1 (0.50)[a]

Table 3. Copy number variation (CNV) of the *CFHR* genes in healthy donors. Results are reported as numeric values (0, 1, 2, etc.), representing the copy number of the gene of interest. n.d: not determined. [a]Previously tested using earlier version of MLPA probe mix (P236-A3 ARMD mix-1) that did not include *CFHR4*[25].

of both FHR-1/1 ($p = 0.0002$) and −1/2 ($p < 0.0001$) compared to FHR-2/2. Interestingly, significantly higher levens of FHR-1/1 versus FHR-1/2 ($p < 0.0001$) and FHR-2/2 ($p < 0.0001$) were observed at 0.063 M sodium chloride.

Reference intervals of FHR-1, -2 and their dimers in healthy donors

Levels of FHR-1, -2 and their homo -and heterodimers were determined in serum of 201 healthy volunteers from the Netherlands. Among them, 96 individuals were newly included in this study, while the remaining 105 individuals had been previously recruited as part of other studies[11,24,25]. In total, 73 (36%) men and 128 (64%) women, with a median age of 45.0 years (CI 42.00–47.00) were tested. In general, males were slightly older (median age: 50.00 years; CI = 41.00–53.00) compared to the females (median age: 43.00 years; CI = 41.00–46.00). Of twelve donors, the age was not known at the time of blood collection.

The copy number variation (CNV) of the *CFH* locus was determined for all donors using MLPA (Table 3). 95 donors were previously determined using an older version (P236-A3 ARMD mix-1) of the MLPA probe mix which did not include *CFHR4,* resulting in missing data for *CFHR4* in these donors. In general, 55 (27.36%) donors tested heterozygous for the *CFHR3/CFHR1* deletion, and eight (3.98%) donors did not have any copies of *CFHR3* and *CFHR1*. These findings align with the expected frequencies observed in the European Caucasian population[26,27]. Next, one donor was found and a second was presumed to be heterozygous for the *CFHR1/CFHR4* deletion, and one donor carried both the *CFHR3/CFHR1* and *CFHR1/CFHR4* deletion, resulting in a

compound heterozygous FHR-1 deficiency. Next, one donor had one copy for *CFHR3*, two copies for *CFHR1* and three copies for *CFHR4*, explained by a *CFHR3/CFHR1* deletion on one allele and a *CFHR1/CFHR4* duplication on the other allele. Lastly, one donor carried a heterozygous duplication of *CFHR3/CFHR1* resulting in three genes copies of *CFHR3* and *CFHR1*.

Consistent with previous findings, the CNV of *CFHR1* had a significant impact on the FHR-1/1 and -2/2 dimer levels (supplemental Table S1, Fig. 4a, b, c)[11]. Specifically, the CNV of *CFHR1* had an inverse proportional effect on FHR-1/1 versus -2/2 levels. Healthy donors with one gene copy for *CFHR1* exhibited lower levels of FHR-1/1 (median = 6.47 µg/mL; CI = 5.78–6.92 µg/mL, $p < 0.0001$) but had higher levels for FHR-2/2 (median = 1.38 µg/mL; CI = 1.13–1.87 µg/mL; $p = 0.0008$) compared to donors with two *CFHR1* gene copies (FHR-1/1 median = 14.18 µg/mL; CI = 13.50–14.75 µg/mL and FHR-2/2 median = 0.98 µg/mL; CI = 0.83–1.29 µg/mL). Similarly, to FHR-1/1, *CFHR1* CNV positively influenced the levels of FHR-1/2 heterodimers. Donors with two copies had significantly more FHR-1/2 (median = 4.89 µg/mL; CI = 4.59–5.29 µg/mL; $p < 0.0001$) than donors with only one gene copy (median = 3.82 µg/mL; CI = 3.30–4.23 µg/mL). As expected, donors that are homozygous for the *CFHR3/CFHR1* deletion had the highest overall levels for FHR-2/2 (median = 4.09 µg/mL; CI = 2.76–4.56 µg/mL; *CFHR1* CNV = 0 vs. 1: $p = 0.0014$, *CFHR1* CNV = 0 vs. 2: $p < 0.0001$). Combining the data from the dimer ELISA's allowed us to calculate total FHR-1 and FHR-2 levels (Table S1,Fig. 4d, e). As expected, CNV of *CFHR1* positively influenced levels of FHR-1 (*CFHR1* CNV = 1, median = 8.81 µg/mL; CI = 7.94–9.48 µg/mL; *CFHR1* CNV = 2, median = 17.21 µg/mL; CI = 16.79–17.65 µg/mL; *CFHR1* CNV = 1 vs. 2: $p < 0.0001$) whereas no significant impact was observed on the level of FHR-2 (*CFHR1* CNV = 0, median = 4.09 µg/mL; CI = 2.76–4.56 µg/mL; *CFHR1* CNV = 1, median = 2.90 µg/mL; CI = 2.43–3.56 µg/mL; *CFHR1* CNV = 2, median = 2.98 µg/mL; CI = 2.65–3.39 µg/mL).

When studying the potential impact of sex and age on protein level (Table S1), results showed no significant impact of gender, but FHR-1/1 homodimers ($r_p = 0.21$; $p = 0.0037$) and the resulting FHR-1 levels ($r_p = 0.21$; $p = 0.0039$), correlated with age.

Next, when correlating FHR-1 and -2 dimers levels independent of CNV (Fig. 4f), results showed a strong correlation between levels of FHR-1, FHR-2 and their homodimers (FHR-1 vs. FHR-1/1: $r_s = 0.98$, $p < 0.0001$; FHR-2 vs. FHR-2/2: $r_s = 0.90$, $p < 0.0001$). Additionally, supported by previous findings, FHR-1/2 levels corrolated stronger with FHR-2 and FHR-2/2 homodimer levels (FHR-1/2 vs. FHR-2: $r_s = 0.91$, $p < 0.0001$; FHR-1/2 vs. FHR-2/2: $r_s = 0.70$, $p < 0.0001$) compared to FHR-1 and FHR-1/1 (FHR-1/2 vs. FHR-1: $r_s = 0.62$, $p < 0.0001$; FHR-1/2 vs. FHR-1/1: $r_s = 0.47$, $p < 0.0001$)[11]. Stratifying based upon *CFHR1* CNV resulted in similar results (supplemental Fig. S3a, b: *CFHR1* CNV = 1: FHR-1/2 vs. FHR-1/1: $r_s = 0.43$, $p = 0.0009$; FHR-1/2 vs. FHR-2/2: $r_s = 0.82$, $p < 0.0001$; *CFHR1* CNV = 2: FHR-1/2 vs. FHR-1/1: $r_s = 0.41$, $p < 0.0001$; FHR-1/2 vs. FHR-2/2: $r_s = 0.90$, $p < 0.0001$), indicating FHR-2 is the main driver in the formation of FHR-1/2 heterodimers.

Lastly, as it is now possible for the first time to directly quantify all FHR-1 and -2 dimer species in parallel, we validated whether FHR-1 and -2 dimerization truly reaches a distribution equilibrium as previously described[11,22]. Based on the level of FHR-1 and -2, the total number of FHR-1 and -2 molecules in circulation was calculated for each individual and used to determine the frequency of FHR-1 and -2. With this, the distribution of FHR-1/1, -1/2, and -2/2 was calculated based on the distribution equilibrium and compared to plasma levels. Results show no significant difference between the predicted and measured levels of FHR-1 and -2 dimers (Fig. 4g).

Genetic determinants regulating systemic FHR-2/2 levels and dictating dimer distribution.

A subset of healthy donors exhibited relatively low FHR-2/2 levels. Through next-generation sequencing (NGS), three low-frequency mutations (c.215G > A, rs79351096; c.595G > T, rs41257904; c.791A > G, rs41310132) and the common SNP rs4085749 (allele frequency: 0.23, European [non-Finnish] population, gnomAD v4) were identified within *CFHR2* (Table 4, Fig. 5a) and associated with altered total levels of FHR-2 (Fig. 5b) and subsequent the levels of FHR-2/2 (Fig. 5e). These mutations have previously been predicted to lead to reduced FHR-2 concentrations based on mRNA expression, inferred FHR-2/2 levels or using mass spectrometry, without addressing FHR-1 and -2 dimer distribution[15,18,21]. Due to the high prevalence of rs4085749 (MAF = 0.325) within the population and the challenges associated with efficiently determining homo- or heterozygosity of the SNP using NGS (due to panel design and high degree of similarity across the *CFH* region), a MLPA probe was developed and confirmed the results found by NGS (supplemental Table S2 and Fig. S3c). When comparing donors lacking the rs4085749 mutation with those who are either heterozygous or homozygous, the significant impact of this common SNP on FHR-1/2 and -2/2 levels was evident (Fig. 5d, e; FHR-1/2: c.420C > T CC vs. CT: $p < 0.0001$; CC vs. TT: $p < 0.0001$; CT vs. TT: $p < 0.0001$; FHR-2/2: c.420C > T CC vs. CT: $p = 0.0008$; CC vs. TT: $p < 0.0001$; CT vs. TT: $p = 0.0069$). Subsequently, the impact of this SNP on total levels of FHR-2 was confirmed (Fig. 5b; c.420C > T CC vs. CT: $p < 0.0001$; CC vs. TT: $p < 0.0001$; CT vs. TT: $p < 0.0001$). As expected, there was no impact on total levels of FHR-1 and FHR-1/1 (Fig. 5c and S3d).

Lastly, the identified low frequency mutations were found to impact FHR-1/2 and FHR-2/2 dimers levels and total levels of FHR-2 to varying extents (Table 4, Fig. 5a, d, e), with combinations of rs41310132 and rs79351096 with the common rs4085749 leading to the overall lowest quantified levels. Consistent with our previous report, a combination of rs79351096 and rs41257904 results in undetectable protein levels[11].

Discussion

The FHRs are hypothesized to act as localized fine tuners of the AP of complement by interfering with the regulatory functions of FH. Previous studies have demonstrated that FHR-1, -2, and FHR-5 form dimers and that dimerization influences their avidity to surface-bound ligands[7,10–13]. Consequently, differences in ligand specificity and affinity among the FHRs involved in dimerization could influence their competition with FH. So far, only FHR-1/1 and -1/2 dimers could be directly determined by ELISA, but the FHR-2/2 dimers have not been quantified and therefore the in vivo distribution of the dimers was unknown.

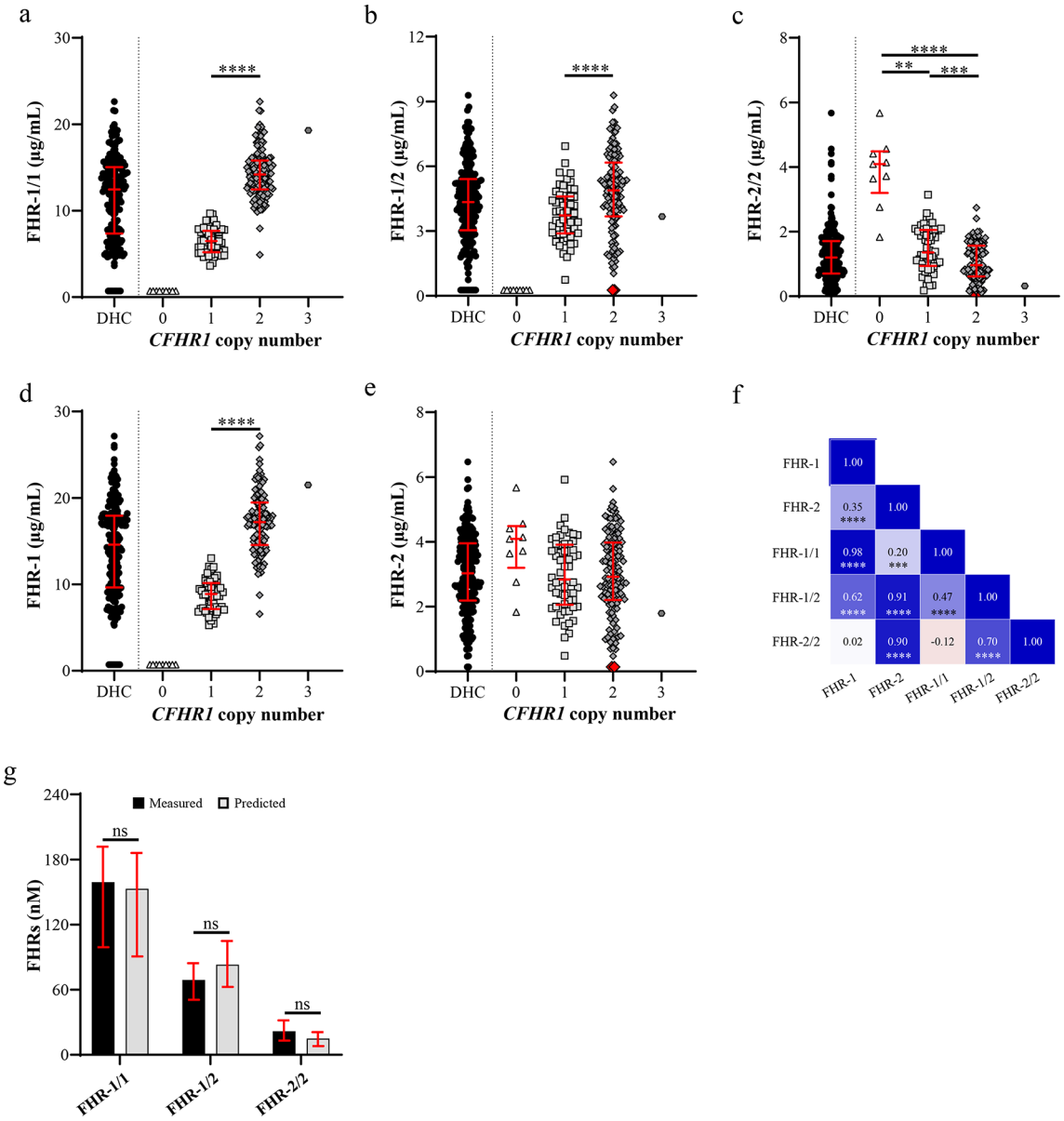

Fig. 4. Reference intervals of FHR-1, -2 and their dimers in healthy donors. Reference levels of (**a**) FHR-1/1, (**b**) FHR-1/2, (**c**) FHR-2/2 and total (calculated) levels of FHR-1 (**d**) and -2 (**e**) in serum of 201 Dutch healthy volunteers. Donors are categorized based on their copy number of *CFHR1* as determined with MLPA. Total levels of FHR-1 and -2 were calculated using measured levels of FHR-1 and -2 dimers. Red colored diamonds are donors identified to lack FHR-2 as previously validated by van Beek et al.[11]. (**f**) Pearson correlation of FHR-1 and -2 and their dimer species. (**g**) Comparison of measured and predicted FHR-1 and -2 dimers in 190 Dutch healthy controls. Predicted levels were determined applying the calculations for when reaching a distribution equilibrium[11,22]. The Shapiro–Wilk test was used to test for normal distribution of the population. (**a**, **b**, **d**) Unpaired t-test with Welch's correction, (**c**) the Kruskal Wallis test, (**e**) the Brown-Forsythe and Welch ANOVA tests, and lastly (**g**) the Chi-squared test were used to test for significant differences. The Dunn's test (**c**) and (**d**) the Dunnett's T3 multiple comparisons test were used to correct for multiple testing. (**a**, **b**, **c**, **d**, **e**) Donors deficient for FHR-1 or lacking FHR-2 were excluded in the statistical analysis. Symbols represent the mean of two measurements with error bars indicating the median with interquartile range. (* $p < 0.05$; ** $p < 0.01$; *** $p < 0.001$; **** $p < 0.0001$).

Directly quantifying FHR-2 homodimer levels has been challenging due to the prevalence of FHR-1/2 heterodimers and the lack of sufficiently sensitive and FHR-2-specific reagents[11]. By using CCP3-4 of FHR-2 as an immunization antigen, we identified five FHR-2 specific monoclonal mAbs and developed an ELISA that specifically detects FHR-2/2 homodimers. This ELISA is based on the same principle as our previously published FHR-1/1 homodimer ELISA, wherein only a homodimer presents a single epitope twice[11]. Interestingly, of the five mAbs identified, only FHR-2.11 could detect FHR-2 homodimers. Possibly, the other mAbs bind to an

CFHR2 exonic variant identified	Chr:bp	Major/minor allele	MAF	Location (aa change)	n of 77	FHR-2 µg/mL (Mean, SD)
Single variants						
rs79351096	1:196,949,611	G/A	0.015	p.Cys72Tyr (CCP1)	3 (Het.)	2.07 (0.16)
rs4085749	1:196,951,018	C/T	0.325	Splice variant (CCP2)	19 (Het.)	2.59 (0.64)
					16 (Hom.)	1.11 (0.22)
rs41257904	1:196,958,055	G/T	0.03	p.Glu199Ter (CCP3)	4 (Het.)	2.10 (0.57)
rs41310132	1:196,959,058	A/G	0.012	p.Tyr264Cys (CCP4)	2 (Het.)	1.69 (0.19)
Combined variants						
rs79351096 & rs41257904	-	-	-	p.Cys72Tyr & p.Glu199Ter[a]	2 (Het. & Het.)	Not detectable
rs79351096 & rs4085749	-	-	-	p.Cys72Tyr & splice variant	2 (Het. & Het.)	0.60 (0.17)
rs41310132 & rs4085749	-	-	-	p.Tyr264Cys & splice variant	1 (Het. & Hom.)	0.48
No variant identified	-	-	-	-	28	4.28 (0.83)

Table 4. Exonic variants in *CFHR2* identified by next-generation sequencing of 77 healthy donors. [a]Donors previous sequenced and typed in van Beek et al.[11]. Het.: heterozygous, Hom.: homozygous, MAF: minor alle frequency.

epitope near the dimerization region of FHR-2, resulting in the formation of monomers and the subsequent loss of the second epitope necessary to detect FHR-2 homodimers. This hypothesis is supported by the selective precipitation of FHR-2 in NHS by these antibodies, without apparent precipitation of FHR-1/2 dimers.

Since FHR-1, -2, and FHR-5 share a high degree of similarity in amino acid sequence and have the ability to form dimers, we rigorously validated the specificity of our FHR-2/2 ELISA using pooled NHS and serum deficient in either FHR-1 or FHR-2 as a source of native protein. By combining antibodies targeting FHR-1 and -5 with our novel FHR-2 antibodies, we confirmed the absence of FHR-1/5 and FHR-2/5 dimers in the serum of healthy donors, addressing a previously debated topic[11,23]. CCP1 and 2 of FHR-5, involved in FHR dimerization, differs slightly from FHR-1 and -2 (Fig. 1a), likely explaining the lack of heterodimers with FHR-1 and FHR-2[10].

Next, using all three FHR-1, -2 dimers ELISAs we further investigated the dynamics and kinetics of dimerization and studied what drives FHR-1 and -2 dimerization. Using FHR-1 or -2 deficient plasma pools that lack FHR-1/2 dimers, we showed a rapid formation of FHR-1/2 in plasma upon incubation at 37 °C that reaches a distribution equilibrium after three hours. This confirms previous results with recombinant human FHR-1 and -2 in a FRET based assay and shows dimerization is an ongoing, dynamic process occurring in plasma[11]. Interestingly, under varying pH levels and sodium chloride concentrations, we observed FHR-1/1 homodimers to be less stable than FHR-1/2 and -2/2 dimers. Although the domains responsible in dimer formation are highly similar between FHR-1 and -2 (CCP1 = 100%, CCP2 = 98%), the small differences in CCP2 could be responsible for this observation[10].

Calibration of the FHR-1/2 heterodimer ELISA proved to be challenging. First, purifying FHR-1/2 from plasma using antibodies is hampered by co-purification of FHR-1/1 and FHR-2/2 dimers. Secondly, given the dynamic nature of dimerization shown here, any purified FHR-1/2 obtained is likely to re-equilibrate into all three dimer species, which leads to a decrease and an unknown FHR-1/2 concentration required for standardization. To overcome this, we leveraged the dynamic characteristic and our homodimer ELISAs to follow the decline in FHR-1/1 and -2/2 levels upon mixing plasma pools deficient in FHR-1 or FHR-2 at 37 °C, and used that to calibrate and establish the concentration of FHR-1/2 in our NHS standard. Using the decline of both homodimers upon mixing FHR-1 and -2 deficient plasma pools, we were able to determine the amount of formed native FHR-1/2. This process was repeated with several mixes of the two deficient plasma pools, each varying in the initial concentrations of FHR-1/1 and -2/2, and all leading to consistent FHR-1/2 levels in our NHS standard. Lastly, by modelling this process we showed an increasing formation of FHR-1/2 formation with a maximum at a molar ratio of 2.25 FHR-1/1 over FHR-2/2, reflecting the normal ratio of FHR-1 and -2 in healthy human plasma.

Futhermore, we directly quantified FHR-2/2 homodimers in serum of healthy donors. Previously, FHR-2/2 levels were inferred based on the measured concentration of FHR-1/1 and -1/2, assuming a distribution equilibrium[11,22]. Although computed versus directly quantified levels strongly correlated (supplemental Fig. S3e), our findings revealed higher levels of FHR-2/2 than previously reported[11]. Minor variations in the calibration of the FHR-1/2 assay by van Beek *et al.* (2017) may have led to the lower inferred FHR-2/2 levels previously reported[11]. Additionally, when calculating total FHR-2 levels, we observed significantly lower levels (median = 3.03 µg/mL; CI = (2.74–3.39) than those recently reported by ELISA (median = 32.1 µg/mL; IQR = 20.0–34.3)[28]. However, specific details on the assay characterization and calibration were not provided in that study. Conversely, mass spectrometry data have reported similar (mean = 3.64 µg/mL; SD = 1.2 µg/mL) or even lower levels (1.20 µg/mL; range = 1.03–1.38) for total FHR-2[15]. Although mass spectrometry offers specificity for protein quantitation by using mass and fragmentation as a fingerprint, this technique is limited in its ability to measure FHR dimer distribution.

Using our complete data on individual dimer levels in 201 healthy donors, we compared their expected distribution of FHR-1 and -2 dimers with directly measured levels. This confirmed that in healthy individuals, FHR-1 and -2 dimerization reaches a distribution equilibrium as previously suggested[11,22]. Knowing this, we further investigated what drives and influences FHR-1 and -2 dimerization. Understanding what drives and

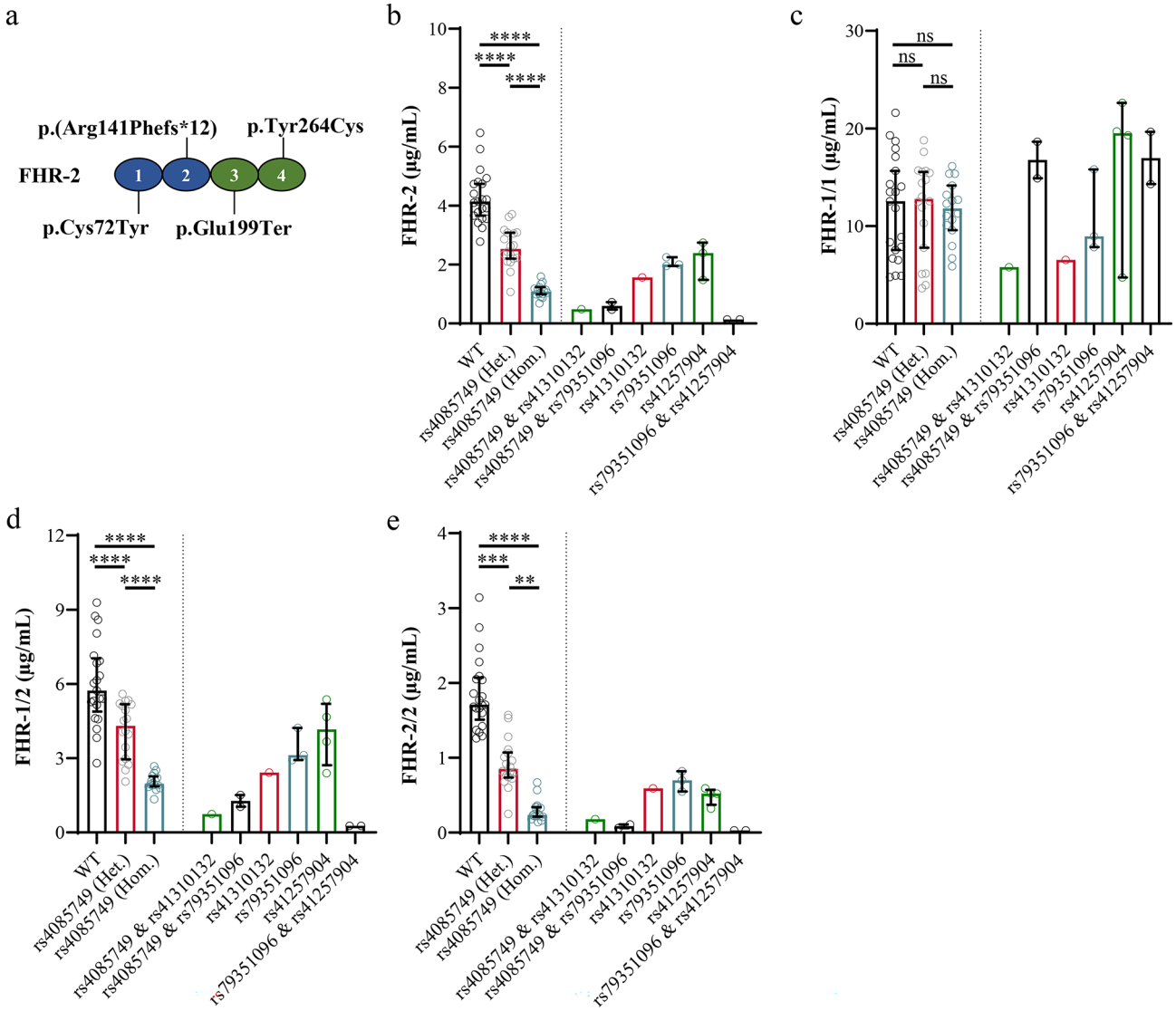

Fig. 5. Genetic determinants in *CFHR2* dictating dimer distribution. Impact of the common SNP rs4085749 and three low frequency SNPs: rs41310132, rs79351096 and rs41257905 on total levels of FHR-2 and FHR-1, -2 dimers in 77 healthy donors. (**a**) Schematic representation of the location and amino acid change of the SNPs within *CFHR2*. (**b**–**e**) Showing the impact of indicated SNPs on total FHR-2, FHR-1/1, -1/2 and -2/2 levels, respectively. (**b**–**e**) The Shapiro–Wilk test was used to test for normal distribution of the population. (**b**, **c**, **d**) The one-way ANOVA test or (**e**) the Kruskal Wallis test was used to test for significant differences. The (**e**) Dunn's test or the (**b**, **c**, **d**) Tukey test were used to correct for multiple testing. Symbols represent the mean of two measurements with error bars indicating the median with interquartile range. (* $p < 0.05$; ** $p < 0.01$; *** $p < 0.001$; **** $p < 0.0001$).

influences FHR-1 and -2 dimerization is important to better understand their role within the complement system and related diseases.

Previously, no impact of age or gender on all three FHR-1 and -2 dimers was observed among children, although significantly lower levels of FHR-1/1 in children compared to adults were reported[19]. In our study, we did observe a correlation of FHR-1/1 and total FHR-1 levels with age, likely driving this significant difference between children and adults.

With the known CNV within the *CFH* locus, and various previously reported SNPs in *CFHR2*, we determined the effect of these genetic variations within Dutch healthy donors on FHR-2/2 levels and the FHR-1 and FHR-2 dimer distribution[11,15,16,18]. As expected, we observed a similar positive effect of the CNV of *CFHR1* on FHR-1/1 levels and confirmed its inverse impact on FHR-2/2 levels[11]. In contrast to previous reports, we observed a significant impact of *CFHR1* CNV on FHR-1/2 levels, likely caused by the larger sample size[11]. FHR-2/2 was found to be the least abundant dimer and showed to be more strongly correlated with FHR-1/2 than FHR-1/1, indicating FHR-2 is the limiting factor for FHR-1/2 formation. We therefore hypothesized that influencing FHR-2 levels will drastically impact FHR-1 and -2 dimer distribution. Previously, several mutation were linked to

reduced FHR-2 levels based upon inferred total levels of FHR-2, mass spectrometry data or by RNA-seq[11,15,16,18]. Specifically, the missense variants rs79351096 (p.Cys72Tyr) and rs41310132 (p.Tyr264Cys) lead to reduced levels due to the presence of free cysteine residues, which subsequently results in aberrant protein formation. The rs41257904 (p.Glu199Ter) results in the loss of FHR-2 CCP4 due to a pre-mature stop codon, resulting in a lack of protein expression. Additionally, rs4085749 creates an alternative splice donor site, which, as shown by liver RNA-seq reads, is preferentially used[18]. This mutation results in the deletion of 12 bases, leading to the loss of a cysteine residue within FHR-2. This loss is hypothesized to significantly impact the protein's structure. We observed a significant decrease in circulating levels of FHR-2/2 and FHR-1/2 but not for FHR-1/1 in healthy donors carrying the aforementioned SNPs. This altered the distribution of FHR-1 and FHR-2 dimers, resulting in a higher ratio of FHR-1/1 homodimers. These findings corroborate FHR-2 is the limiting factor for FHR-1/2 formation. Previously, the identified low frequency *CFHR2* mutations were associated with lower inferred FHR-2 levels, which in turn showed to be protective for advanced AMD[16]. Here, we confirm the association between these low frequency mutations and protein levels with directly measured FHR-2/2. Interestingly, levels of the low frequency mutations were found to be similar to those for the more common SNP rs4085749. As the later mutation is not associated with AMD, and the low frequency mutations are all present in heterozygous state, further research is needed to validate whether the reported associations with AMD are truly driven by protein levels of FHR-2 or by a specific genotype on the other chromosome.

Although FHR-1 and FHR-2 share high similarity, research has demonstrated differences in their ligand-binding properties as reviewed by Lucientes-Continente et al.[29]. As dimerization influences the avidity of these proteins towards surface-bound ligands, it likely impacts their direct competition with FH and its regulatory functions in the complement system. With diseases as AMD, aHUS, C3-glomerulopathy and ANCA vasculitis having a clear link with FHR-1 and -2[13,16–18,30]. Being able to directly quantify each FHR-1 and -2 dimer and understand their distribution, we can now explore the functional consequences of the different FHR dimer species in fine-tuning complement in both health and disease.

Materials and methods

Blood samples

Serum and plasma samples were collected from anonymous healthy volunteers with written consent according to Dutch regulations and the Declaration of Helsinki. Before collecting the serum, blood was clotted for one hour at room temperature (RT). Serum and plasma were obtained after centrifugation at 1600 × g at 4 °C for ten minutes. In addition, the peripheral blood mononuclear cell fraction of the EDTA sample was collected for DNA extraction using the QIAamp DNA blood Mini Kit (Qiagen, Hilden, Germany) according to manufacturer's instructions. All samples were aliquoted and stored at – 80 °C until use. Healthy donors deficient for FHR-2 were previously described[11]. Healthy donors deficient for FHR-1 (due to deletion of *CFHR3/CFHR1* and/or *CFHR1/CFHR4*) were identified by MLPA and confirmed by ELISA (described below).

MLPA and next generation sequencing

Copy number variation (CNV) in the *CFH* locus was determined by multiplex ligation-dependent probe amplification (MLPA) according to manufacturer's instructions[25,31–34]. Results are reported as numeric values (0, 1, 2, etc.), representing the copy number of the gene of interest. The *CFH* salsa probe mix P236-B1 (MRC holland, Amsterdam, The Netherlands) and an in house designed synthethic probe (supplemental Table S2, obtained from Integrated DNA Technologies, Coralville, Iowa, USA) to detect the SNP rs4085749, were used to genotype the *CFH* region according to manufacturer's instructions. Additionally, the *CFH* locus of a random selection of 77 healthy donors was sequenced using the custom-made Ampliseq complement panel (Sanquin Complement Panel, Thermo Fisher Scientific)[35]. DNA library preparation and sequencing was performed according to manufacturer protocols using a Ion Chef™ and Ion S5™ system (Thermo Fisher Scientific). Sequence data was analysed using Ion Reporter software workflow 5.16 (Thermo Fisher Scientific).

Production of recombinant proteins

Recombinant human FHR (rhFHR) -1, -2, -3, -4A and FHR-5, monomeric rhFHR-1 and the rhFHR-2 antigen used for mouse immunizations were expressed and purified based on the protocol of Vink *et al.* 2014 with a minor adjustment[36,37]. Four hours post transfection, 10% (v/v) primatone RL (Sigma Aldrich, Saint Louis, Missouri, USA) was added to improve cell culture performance. The purity of the final product after IMAC purification using a HisTrap™ column (GE Healthcare, Chicago, Illinois, USA) was evaluated using SDS-PAGE under non-reducing conditions and stained using InstantBlue® Coomassie Protein Stain (Abcam, Waltham, Boston) according to manufacturer's instructions. When indicated, purified proteins and antibodies were biotinylated using EZ-Link™ Sulfo-NHS-LC-Biotin (Thermo Fisher Scientific, cat. #A39257, Massachusetts, USA) according to manufacturer's instructions.

Mouse immunisations and hybridoma formation

All animal procedures were carried out in accordance with the international standards for human care and use of laboratory animals. Ethical approval in adherence to the ARRIVE guidelines was approved by the central committee for animal use and IVD of the Netherlands Cancer Institute, Amsterdam, The Netherlands. To generate anti-FHR-2 antibodies, Balb/c mice (Jackson Laboratory) were immunized by I.P. injection of 200 µL containing rhFHR-2 CCP3-4 (0.125 mg/mL, PBS) in 50% (v/v) Montanide ISA V50 V2 (Seppic, La Garenne-Colombes, France). A first booster was given after four weeks, followed two weeks later by the final booster. Three days after the last booster, spleen and lymph nodes were isolated and processed to obtain single cells. Cells were than fused as described in Hoekzema et al.[39] with the mouse myeloma SP2/0 cell line in a 3:1 ratio using 42% (v/v) Polyethylene glycol 4000 (Merck cat #9727, Rahway, New Jersey, USA) to generate hybridomas

and cultured under hybridoma-selecting conditions (IMDM medium supplemented with 1% (v/v) Penicillin/Streptomycin (Invitrogen, Waltham, Massachusetts, USA), 5% (v/v) fetal calf serum (Bodinco, Alkmaar, The Netherlands), 0.5 ng/mL recombinant human IL-6 (in house produced and described by Rispens *et al.*, (2011) and 50 µM β-mercaptoethanol (Merck Millipore, Darmstadt, Germany), 0.1 mM hypoxanthine (Sigma Aldrich) and 1 µg/mL azaserine (Sigma Aldrich)[38,39]. Only hybridomas producing antibodies with apparent rhFHR-2 specificity (tested as described below) were selected and made monoclonal through multiple limiting dilution cultures. Monoclonal hybridomas were cultured in IMDM medium supplemented with 1% (v/v) Penicillin/Streptomycin, 2.5% (v/v) fetal calf serum, 0.5 ng/mL IL-6 and 50 µM β-mercaptoethanol for up to four weeks, depending on the culture volume. Next, mAbs were purified using a HiTrap® Protein A High Performance 1 mL column (GE Healthcare, Chicago, Illinois, USA) according to the manufacturer's instructions. Lastly, antibody isotype was determined using an IsoStrip™ mouse mAb isotyping kit (Roche, Basel, Switzerland) according to the manufacturer's instructions.

ELISAs

For all ELISAs, catching antibodies were coated overnight at RT on Nunc MaxiSorp™ 96-wells micro titre plates (Invitrogen). Incubation steps were performed at RT whilst shaking unless stated otherwise. After each incubation step, plates were washed five times with PBS containing 0.02% (v/v) Tween®-20 (PT) using a microplate washer (BioTek 405 LSRS , BioTek Instruments, Winooski, VT, USA). Assays were developed using ready-to-use 3,3',5,5' tetramethylbenzidine solution (TMB, Thermo Fisher Scientific, cat. #34,029,) diluted to 50% (v/v) in milli Q water. The reaction was stopped by the addition of 0.2 M H_2SO_4. All steps were performed with a volume of 100 µL per well. Absorbance was measured at 450 nm using a Synergy 2 plate reader (BioTek Instruments, Winooski, USA) and corrected for background absorbance at 540 nm.

Identification of monospecific anti-FHR-2 antibody producing hybridoma's

Mouse kappa immunoglobulins present in the culture supernatant (20% (v/v), diluted in PT0.2%) were captured on rat anti-mouse RM-19 (3 µg/mL diluted in PBS, Sanquin Research, Amsterdam, The Netherlands) coated plates. Simultaneously, 0.2 µg/mL biotinylated full length wild type rhFHR-2 was added and incubated for one hour. Lastly, plates were incubated for 30 min with 0.05% (v/v) HRP-conjugated streptavidin (strep-HRP, GE Healthcare, cat. #RPN1231, Chicago Illinois USA) diluted in PT0.1% and developed as described above.

Similarly, the culture supernatant of hybridoma's positive for the production of αFHR-2 antibodies was used in an initial antibody specificity screening. In short, RM-19 coated plates were incubated with culture supernatant (10%, v/v) and biotinylated plasma-derived FH (pdFH, Complement technologies, Texas, USA) and rhFHR-1, -2, -3, -4A and -5 (0.2 µg/mL) diluted in high performance ELISA buffer (HPE, Essange Reagents, Amsterdam, The Netherlands). Afterwards, plates were incubated for 30 min with strep-HRP (0.05% (v/v), in PT0.1%) and developed as described above.

Cross-reactivity for FH family members

Plates coated with 2 µg/mL purified mAbs diluted in PBS were incubated with biotinylated pdFH, rhFHR-1, -2, -3, -4A and -5 (10 nM) diluted in HPE. After washing, plates were incubated with 0.01% (v/v) strep-poly-HRP (Essange Reagents, Amsterdam, The Netherlands) diluted in PT0.1% and developed as described above.

Competition ELISA

αFHR-2 mAbs were tested for competing for epitope binding using biotynilated rhFHR-2. Each αFHR-2 mAb was coated on Nunc Maxisorp 96-well microtiter plates at 2 µg/mL diluted in PBS. Biotynilated rhFHR-2 (0.1 µg/mL, in HPE) was pre-incubated with αFHR-2 mAbs (10 µg/mL, in HPE) for twenty minutes before adding to the ELISA plate for one hour. Next, wells were incubated with 0.01% (v/v) streptavidin poly-HRP for thirty minutes before being developed as described above. Binding of biotinylated rhFHR-2 was expressed as relative binding of biotinylated rhFHR-2 in the presence of an isotype control.

FHR-1 and -2 hetero -and homodimer ELISAs

FHR-1 homodimers were quantified as previously described[11]. To determine FHR-1/2 heterodimers, plates were coated with αFHR-2.11 (2 µg/mL in 0.1 M carbonate-bicarbonate buffer, pH 9.6). Samples were diluted in HPE and incubated at RT for one hour. Next, FHR-1/2 heterodimers were detected using the biotinylated mAb αFH.02 (FH mAb cross-reactive for FHR-1, 0.25 µg/mL in HPE) for one hour before being incubated with 0.05% (v/v) strep-HRP in PT0.1% for 30 min. Lastly, plates were developed as described above[23].

Similarly, FHR-2 homodimers were measured by coating αFHR-2.11 (1 µg/mL in 0.1 M carbonate-bicarbonate buffer, pH 9.6). After sample incubation (diluted in HPE) of one hour, homodimers were detected using biotinylated αFHR-2.11 (0.125 µg/mL in HPE) whereafter plates were incubated with 0.001% (v/v) strep-poly-HRP diluted in PT0.1% and developed as described above.

To ensure assay reproducibility and data reliability. Each blood donor was measured twice on separate ELISA plates using two dilutions. For each sample, the coefficient of variation (CV) was calculated. A CV below 15% was required for results to be considered reliable. The Inter-assay variation was determined to be on average 11% for FHR-1/1, 7% for FHR-1/2 and 9% for FHR-2/2 based on three control samples that were included on all ELISA plates and measured at least 20 times. Protein levels are expressed in µg/mL and were calculated using a calibrated standard curve of a normal human serum pool (NHS; > 400 donors, kindly provided by Sanquin Diagnostic Services, Amsterdam, The Netherlands).

Calibration FHR-1/2 and FHR-2/2 ELISA

The concentration of FHR-2/2 in our NHS standard was set using rhFHR-2, of which the concentration was determined via nanodrop (NanoDrop One, ThermoFisher Scientific) using an extinction coefficient of 1.62 (280 nm, 0.1%, w/v, including 6xHis-tag). To calibrate the FHR-1/2 ELISA, sera deficient for either FHR-1 or -2 were mixed in various ratios (100–0%, 95–5%, 85–15%, 75–25%, 50–50%, 25–75%, 15–85%, 5–95% and 0–100% (v/v) FHR-2 deficient and *CFHR3/CFHR1* deficient EDTA plasma, respectively), with a total volume of 300 µL and incubated for six hours at 37 °C to allow FHR-1/2 formation. The plasma samples used for calibration were specifically selected to be deficient in either FHR-1 or FHR-2. The FHR-1 deficient plasma served as a source of FHR-2/2, while the FHR-2 deficient plasma provided FHR-1/1. Next, concentration of the formed FHR-1/2 heterodimers was determined by measuring the remaining FHR-1 and -2 homodimers by ELISA as described above. The mixtures, now with a known amount of native FHR-1/2 heterodimers, were used to calibrate the NHS standard.

Investigating dimer kinetics and dimer strength

To study the kinetics of dimer formation, equimolar amounts of native FHR-1 and -2 in EDTA plasma deficient in either FHR-1 or -2 were incubated for a range of time points (zero minutes to overnight) at 37 °C. After incubation, samples were immediately placed on melting ice to halt further dimerization. Next, levels of formed FHR-1/2 heterodimers were determined as described above, with the difference that the sample incubation was carried out on melting ice.

To investigate the impact of pH on homo- and heterodimers, NHS was incubated at pH 6.5 to 9.0. Citric acid monohydrate (Merck Millipore) and 1,3-Bis[tris(hydroxymethyl)methylamino]propane (CBTP, Sigma Aldrich), both 40 mM prepared in an isotonic solution (Versylene® Fresenius, NaCl 0.9%, Fresenius Kabi, Serves, France) containing 0.02% (v/v) Tween®-20 and 0.3% (w/v) BSA (Sigma Aldrich), were used to prepare the pH range. FHR dimer ELISA's were performed as described above with the only difference the incubation of serum at various pH conditions.

The FHR-1 and -2 dimers were further investigated by adding sodium chloride at indicated final concentrations (0.0625–2 M) during the sample step. FHR dimer assays were conducted and developed as previously described. Possible direct effects of this pH range or the sodium chloride concentration on antibody-antigen binding capacity was excluded using recombinant monomeric FHR proteins (supplemental Fig. 2 a, b).

Immunoprecipitation

FHR proteins were precipitated from a NHS pool or serum deficient either in FHR-1 (*CFHR3/CFHR1* deficient serum determined via MLPA) or -2 (previously determined via gene sequencing) as previously described[11]. Following Western blotting, membranes were stained for one hour with 1 µg/mL biotinylated αFHR-2.1 (FHR-1, FHR-2), αFHR-5.4 (FHR-5), αFHR-3.1 (FHR-3, FHR-4) or αFH.16 (FH) to detect the FH protein family[11,23,25]. Blots were developed using ECL (Thermo Fisher Scientific) and imaged on a Chemidoc™ MP System (BioRad, Hercules, CA, USA), and analysed using ImageLab software version 6.0 (BioRad).

Statistics

Data and statistical analysis were conducted using GraphPad Prism version 9.1.1 for Windows (GraphPad Software, San Diego, California USA). Before testing significance, a Shapiro–Wilk test was performed to test for normal distribution. The Mann–Whitney, Welch's t-test, Kruskal–Wallis, one way ANOVA, Brown-Forsythe and Welch ANOVA, Chi square test and the Friedman test were used to assess significant differences as indicated, with p-values below 0.05 indicating statistical significance. Were needed, appropriate correction for multiple testing was applied. The parametric Pearson and non-parametric Spearman correlation test were used to evaluate correlations.

Data availability

The dataset generated and analysed during the current study is provided within the manuscript or supplementary information files.

Received: 18 July 2024; Accepted: 11 March 2025
Published online: 28 March 2025

References

1. Merle, N. S., Church, S. E., Fremeaux-Bacchi, V. & Roumenina, L. T. Complement system part I—molecular mechanisms of activation and regulation. *Front. Immunol.* **6**(JUN), 1–30. https://doi.org/10.3389/fimmu.2015.00262 (2015).
2. Zipfel, P. F. & Skerka, C. Complement regulators and inhibitory proteins. *Nat. Rev. Immunol.* **9**(10), 729–740. https://doi.org/10.1038/nri2620 (2009).
3. Parente, R., Clark, S. J., Inforzato, A. & Day, A. J. Complement factor H in host defense and immune evasion. *Cell. Mol. Life Sci.* **74**(9), 1605–1624. https://doi.org/10.1007/s00018-016-2418-4 (2017).
4. Józsi, M., Schneider, A. E., Kárpáti, É. & Sándor, N. Complement factor H family proteins in their non-canonical role as modulators of cellular functions. *Semin. Cell Dev. Biol.* https://doi.org/10.1016/j.semcdb.2017.12.018 (2019).
5. Krushkal, J., Bat, O. & Gigli, I. Evolutionary relationships among proteins encoded by the regulator of complement activation gene cluster. *Mol. Biol. Evol.* **17**(11), 1718–1730. https://doi.org/10.1093/OXFORDJOURNALS.MOLBEV.A026270 (2000).
6. Cantsilieris, S. et al. Recurrent structural variation, clustered sites of selection, and disease risk for the complement factor H (CFH) gene family. *Proc. Natl. Acad. Sci. USA* **115**(19), E4433–E4442. https://doi.org/10.1073/pnas.1717600115 (2018).
7. Tortajada, A. et al. C3 glomerulopathy–associated CFHR1 mutation alters FHR oligomerization and complement regulation. *J. Clin. Invest.* **123**(6), 2434–2446. https://doi.org/10.1172/JCI68280 (2013).
8. Józsi, M., Tortajada, A., Uzonyi, B., Goicoechea de Jorge, E. & Rodríguez de Córdoba, S. Factor H-related proteins determine complement-activating surfaces. *Trends Immunol.* **36**(6), 374–384. https://doi.org/10.1016/j.it.2015.04.008 (2015).

9. Sánchez-Corral, P., Pouw, R. B., López-Trascasa, M. & Józsi, M. Self-damage caused by dysregulation of the complement alternative pathway: Relevance of the factor H protein family. *Front. Immunol.* **9**(JUL), 1–19. https://doi.org/10.3389/fimmu.2018.01607 (2018).
10. Goicoechea De Jorge, E. et al. Dimerization of complement factor H-related proteins modulates complement activation in vivo. *Proc. Natl. Acad. Sci. USA* https://doi.org/10.1073/pnas.1219260110 (2013).
11. van Beek, A. E. et al. Factor H-related (FHR)-1 and FHR-2 form homo- and heterodimers, while FHR-5 circulates only as homodimer in human plasma. *Front. Immunol.* https://doi.org/10.3389/fimmu.2017.01328 (2017).
12. Csincsi, Á. I. et al. FHR-1 binds to C-reactive protein and enhances rather than inhibits complement activation. *J. Immunol.* **199**(1), 292–303. https://doi.org/10.4049/jimmunol.1600483 (2017).
13. Marquez-Tirado, B. et al. Factor H-related protein 1 drives disease susceptibility and prognosis in C3 glomerulopathy. *J. Am. Soc. Nephrol.* **33**(6), 1137–1153. https://doi.org/10.1681/ASN.2021101318 (2022).
14. Banerjee, P. et al. Evaluating the clinical utility of measuring levels of factor H and the related proteins. *Mol. Immunol.* **151**, 166–182. https://doi.org/10.1016/J.MOLIMM.2022.08.010 (2022).
15. Cipriani, V. et al. Beyond factor H: The impact of genetic-risk variants for age-related macular degeneration on circulating factor-H-like 1 and factor-H-related protein concentrations. *Am. J. Hum. Genet.* **108**(8), 1385–1400. https://doi.org/10.1016/j.ajhg.2021.05.015 (2021).
16. Lorés-Motta, L. et al. Common haplotypes at the CFH locus and low-frequency variants in CFHR2 and CFHR5 associate with systemic FHR concentrations and age-related macular degeneration. *Am. J. Human Genetics* **108**(8), 1367–1384. https://doi.org/10.1016/J.AJHG.2021.06.002 (2021).
17. Hughes, A. E. et al. A common CFH haplotype, with deletion of CFHR1 and CFHR3, is associated with lower risk of age-related macular degeneration. *Nat. Genetics* **38**(10), 1173–1177. https://doi.org/10.1038/ng1890 (2006).
18. Hughes, A. E. et al. Sequence and expression of complement factor H gene cluster variants and their roles in age-related macular degeneration risk. *Invest. Ophthalmol. Vis. Sci.* **57**(6), 2763–2769. https://doi.org/10.1167/iovs.15-18744 (2016).
19. van Beek, A. E. et al. Reference intervals of factor H and factor H-related proteins in healthy children. *Front. Immunol.* **9**(AUG), 1–6. https://doi.org/10.3389/fimmu.2018.01727 (2018).
20. van Beek, A. E. et al. Low levels of factor H family proteins during meningococcal disease indicate systemic processes rather than specific depletion by *Neisseria meningitidis*. *Front. Immunol.* https://doi.org/10.3389/FIMMU.2022.876776 (2022).
21. Lorés-Motta, L. et al. Common haplotypes at the CFH locus and low-frequency variants in CFHR2 and CFHR5 associate with systemic FHR concentrations and age-related macular degeneration. *Am. J. Hum. Genet.* **108**(8), 1367–1384. https://doi.org/10.1016/j.ajhg.2021.06.002 (2021).
22. Rispens, T., Ooijevaar-De Heer, P., Bende, O. & Aalberse, R. C. Mechanism of immunoglobulin G4 Fab-arm exchange. *J. Am. Chem. Soc.* **133**(26), 10302–10311. https://doi.org/10.1021/JA203638Y (2011).
23. Pouw, R. B. et al. Potentiation of complement regulator factor H protects human endothelial cells from complement attack in aHUS sera. *Blood Adv.* **3**(4), 621–632. https://doi.org/10.1182/bloodadvances.2018025692 (2019).
24. Pouw, R. B. et al. Complement factor H-related protein 4A is the dominant circulating splice variant of CFHR4. *Front. Immunol.* https://doi.org/10.3389/fimmu.2018.00729 (2018).
25. Pouw, R. B. et al. Complement factor H-related protein 3 serum levels are low compared to factor H and mainly determined by gene copy number variation in CFHR3. *PLoS One* **11**(3), 1–13. https://doi.org/10.1371/journal.pone.0152164 (2016).
26. Holmes, L. V. et al. Determining the population frequency of the CFHR3/CFHR1 deletion at 1q32. *PLoS One.* **8**(4), e60352. https://doi.org/10.1371/JOURNAL.PONE.0060352 (2013).
27. Moore, I. et al. Association of factor H autoantibodies with deletions of CFHR1, CFHR3, CFHR4, and with mutations in CFH, CFI, CD46, and C3 in patients with atypical hemolytic uremic syndrome. *Blood* **115**(2), 379–387. https://doi.org/10.1182/blood-2009-05-221549 (2010).
28. Lucientes-Continente, L. et al. Complement alternative pathway determines disease susceptibility and severity in antineutrophil cytoplasmic antibody (ANCA)–associated vasculitis. *Kidney Int.* **105**(1), 177–188. https://doi.org/10.1016/j.kint.2023.10.013 (2024).
29. Lucientes-Continente, L., Márquez-Tirado, B. & Goicoechea de Jorge, E. The Factor H protein family: The switchers of the complement alternative pathway. *Immunol. Rev.* **313**(1), 25–45. https://doi.org/10.1111/IMR.13166 (2023).
30. Irmscher, S. et al. Serum FHR1 binding to necrotic-type cells activates monocytic inflammasome and marks necrotic sites in vasculopathies. *Nat. Commun.* https://doi.org/10.1038/s41467-019-10766-0 (2019).
31. Hebecker, M. & Józsi, M. Factor H-related protein 4 activates complement by serving as a platform for the assembly of alternative pathway C3 convertase via its interaction with C3b protein. *J. Biol. Chem.* **287**(23), 19528–19536. https://doi.org/10.1074/JBC.M112.364471 (2012).
32. Mihlan, M. et al. Human complement factor H-related protein 4 binds and recruits native pentameric C-reactive protein to necrotic cells. *Mol. Immunol.* https://doi.org/10.1016/j.molimm.2008.10.029 (2009).
33. Tortajada, A. et al. Elevated factor H-related protein 1 and factor H pathogenic variants decrease complement regulation in IgA nephropathy. *Kidney Int.* **92**(4), 953–963. https://doi.org/10.1016/J.KINT.2017.03.041 (2017).
34. Schäfer, N. et al. Complement regulator FHR-3 Is elevated either locally or systemically in a selection of autoimmune diseases. *Front. Immunol.* **7**, 542. https://doi.org/10.3389/fimmu.2016.00542 (2016).
35. Kuijpers, T. W. et al. Combined immunodeficiency with severe inflammation and allergy caused by ARPC1B deficiency. *J. Allerg. Clin. Immunol.* **140**(1), 273-277.e10. https://doi.org/10.1016/J.JACI.2016.09.061 (2017).
36. Marquez-Tirado, B. et al. Factor H-related protein 1 drives disease susceptibility and prognosis in C3 glomerulopathy. *J. Am. Soc. Nephrol.* **33**(6), 1137–1153. https://doi.org/10.1681/ASN.2021101318/-/DCSUPPLEMENTAL (2022).
37. Vink, T., Oudshoorn-Dickmann, M., Roza, M., Reitsma, J. J. & de Jong, R. N. A simple, robust and highly efficient transient expression system for producing antibodies. *Methods* **65**(1), 5–10. https://doi.org/10.1016/J.YMETH.2013.07.018 (2014).
38. Rispens, T. et al. Label-free assessment of high-affinity antibody–antigen binding constants. Comparison of bioassay, SPR, and PEIA-ellipsometry. *J. Immunol. Methods* **365**(1–2), 50–57. https://doi.org/10.1016/J.JIM.2010.11.010 (2011).
39. Hoekzema, R., Martens, M., Brouwer, M. C. & Hack, C. E. The distortive mechanism for the activation of complement component C1 supported by studies with a monoclonal antibody against the "arms" of C1q. *Mol. Immunol.* **25**(5), 485–494. https://doi.org/10.1016/0161-5890(88)90169-1 (1988).

Author contributions

B.R.J.V., T.W.K., and R.B.P. designed the research. B.R.J.V., M.C.B., and G.V.M. conducted experiments and gathered data. J.G., K.V.L., M.D. and N.K. genotyped healthy donors and analysed the data. B.R.J.V. and M.K. performed animal experiments. B.R.J.V. and R.B.P.: analysed data and drafted the manuscript. All authors critically reviewed the manuscript and approved the final version for publication. They agreed to be accountable for all aspects of the work, ensuring that questions related to the accuracy or integrity of any part of the work are appropriately investigated and resolved.

Funding
This research was supported by the European Union's Horizon 2020 research and innovation program under grant agreement No. 899163 (SciFiMed) and by the Sanquin Research Fund Young Investigator Award to BRJV. The funding agencies had no role in the study design, data interpretation, or decision to publish.

Declarations

Competing interests
MCB, TWK and RBP are co-inventors of patents and patents applications describing potentiating anti-FH antibodies and uses thereof. All other authors declare no conflict of interest.

Ethical approval
After consultation with the ethical board of Sanquin Research, Amsterdam, The Netherlands, a system was established for obtaining blood samples for scientific research (no approval number available). This volunteer system is organized according to Dutch regulations and according to the Declaration of Helsinki. This volunteer system certifies, among others, that: Blood samples used for scientific studies by researchers of the Sanquin Research department were drawn from healthy, anonymized volunteers with written informed consent; No personal characteristics of the volunteers are registered; The volunteers nor those taking the samples know for what project specific samples are used; Allowed annual sample volume and frequency of donation were established after consultation with Sanquin Medical Secretary. Standard operating procedures are available upon request.

Additional information
Supplementary Information The online version contains supplementary material available at https://doi.org/10.1038/s41598-025-94064-4.

Correspondence and requests for materials should be addressed to R.B.P.